Pyrene-labeled gangliosides: Micelle formation in aqueous solution, lateral diffusion, and thermotropic behavior in phosphatidylcholine bilayers

ARTICLE *in* BIOCHEMISTRY · OCTOBER 1987

Impact Factor: 3.02 · DOI: 10.1021/bi00392a055 · Source: PubMed

4 AUTHORS, INCLUDING:

Günter Schwarzmann
University of Bonn
112 PUBLICATIONS **5,086** CITATIONS
SEE PROFILE

Hans-Joachim Galla
University of Münster
360 PUBLICATIONS **11,076** CITATIONS
SEE PROFILE

Parodi, A. J., Martin-Barrientos, J., & Engel, J. C. (1984) *Biochem. Biophys. Res. Commun. 118*, 1–7.
Previato, J. O., Mendelzon, D. H., & Parodi, A. J. (1986) *Mol. Biochem. Parasitol. 18*, 343–353.
Rearick, J. I., Chapman, A., & Kornfeld, S. (1981a) *J. Biol. Chem. 256*, 6255–6261.
Rearick, J. I., Fujimoto, K., & Kornfeld, S. (1981b) *J. Biol. Chem. 256*, 3762–3769.
Sharma, C. B., Babczinski, P., Lehle, L., & Tanner, W. (1974) *Eur. J. Biochem. 46*, 35–41.
Spiro, M. J., Spiro, R. G., & Bhoyroo, V. D. (1979) *J. Biol. Chem. 254*, 7668–7674.
Staneloni, R. J., Ugalde, R. A., & Leloir, L. F. (1980) *Eur. J. Biochem. 105*, 275–278.
Staneloni, R. J., Tolmasky, M. E., Petriella, C., & Leloir, L. F. (1981) *Plant Physiol. 68*, 1175–1179.
Stoll, J., Robbins, A. R., & Krag, S. S. (1982) *Proc. Natl. Acad. Sci. U.S.A. 79*, 2296–2300.
Taniguchi, T., Mizuochi, T., Banno, Y., Nozawa, Y., & Kobata, A. (1985) *J. Biol. Chem. 260*, 13941–13946.
Turco, S. J., Stetson, B., & Robbins, P. W. (1977) *Proc. Natl. Acad. Sci. U.S.A. 74*, 4411–4414.
Wright, A., & Robbins, P. W. (1965) *Biochim. Biophys. Acta 104*, 594–596.

Pyrene-Labeled Gangliosides: Micelle Formation in Aqueous Solution, Lateral Diffusion, and Thermotropic Behavior in Phosphatidylcholine Bilayers†

Marika Ollmann,‡ Günter Schwarzmann,§ Konrad Sandhoff,§ and Hans-Joachim Galla*,‡
Institut für Biochemie, Technische Hochschule Darmstadt, D-6100 Darmstadt, FRG, and Institut für Organische Chemie und Biochemie, Universität Bonn, D-5300 Bonn, FRG

Received February 10, 1987; Revised Manuscript Received May 1, 1987

ABSTRACT: By use of the excimer technique, the formation in aqueous solution of pyrene-labeled ganglioside micelles and their lateral diffusion and distribution in phosphatidylcholine membranes were investigated. For these studies 12-(1-pyrenyl)dodecanoic acid was covalently attached to the ceramide part of lysogangliosides G_{M1}, G_{M2}, G_{M3}, G_{D1a}, and G_{D1b}. The 12-(1-pyrenyl)dodecanoic acid substitute of phosphatidylcholine was used for comparison. All pyrene-labeled gangliosides were present in aqueous solution in a predominantly micellar form down to 2×10^{-8} M, which is the technical limit of this method. The tendency to aggregate is highest for PyG_{D1a} and PyG_{D1b}. In fluid dipalmitoylphosphatidylcholine bilayers the excimer-to-monomer fluorescence intensity ratio of pyrene-labeled gangliosides PyC_{M1}, PyG_{M2}, PyG_{M3}, PyG_{D1a}, and PyG_{D1b} increases linearly with ganglioside concentration. The calculated diffusion coefficients for gangliosides are comparable to 1.6×10^{-7} cm^2/s, which is the diffusion coefficient of pyrene-labeled phosphatidylcholine [Galla, H.-J., & Hartmann, W. (1980) *Chem. Phys. Lipids 27*, 199–219]. In comparison to phosphatidylcholine, the diffusion of monosialogangliosides is slightly increased, with that diffusion of disialogangliosides being slightly decreased. Ca^{2+} ions up to 200 mM do not affect ganglioside diffusion significantly. The shape of the lipid phase transition curves obtained by the excimer technique yields information on the lateral distribution of the tested probe molecules. Pyrene-labeled phosphatidylcholine was taken as reference for a system with complete miscibility but nonideal mixing. 1-Acyl-2-[10-(1-pyrenyl)decanoyl]-*sn*-glycero-3-phosphocholine (PyPC) is known to be randomly distributed in the gel and in the fluid-crystalline lipid phase of dipalmitoylphosphatidylcholine bilayer membranes. It distributes preferentially into the fluid phase in the phase-transition region. In comparison, PyPC in dimyristoylphosphatidylcholine membranes is an example of a system with nearly ideal mixing [Hresko, R. C., Sugar, J. P., Barenholz, Y., & Thompson, T. E. (1986) *Biochemistry 25*, 3813–3828]. Phase-transition curves of pyrene-labeled gangliosides exemplify a nearly ideal mixing system with PyG_{D1a} or PyG_{D1b} producing best effects. The monosialogangliosides, however, exhibit less ideality of mixing, the deviation from an ideal mixing behavior increasing with decreasing number of both neutral sugar residues and sialic acid groups. Addition of Ca^{2+} triggers a tightening of the phosphatidylcholine bilayer and thus induces a change in the lateral distribution of the gangliosides at the phase transition. The system passes into a nonideal mixture, which holds true for PyG_{M3} and PyG_{M2} though less so for PyG_{M1}. PyG_{D1a} and PyG_{D1b} exhibit almost ideal mixing even in the presence of 200 mM Ca^{2+}. This clearly demonstrates that the favorable interaction of G_{D1a} or G_{D1b} with phosphatidylcholine is due to a better fit of the head group dipoles, as was postulated by Maggio et al. [Maggio, B., Cumar, F. A., & Caputto, R. (1980) *Biochem. J. 189*, 435–440]. This Ca^{2+} effect slightly below the phase-transition temperature of the host lipid is time dependent. The increase in excimer formation of pyrene-labeled gangliosides is immediate with concentrations up to 100 mM. However, above this Ca^{2+} concentration the immediate response is followed by a prolonged increase.

Gangliosides are sialic acid containing glycosphingolipids which are minor but essential components of the vertebrate plasma membrane. In extraneural tissue gangliosides are implicated in various surface recognition and physiological processes. For example, G_{M1} and G_{M3} have been shown to regulate cell proliferation. Moreover, G_{M1} and G_{M3} control ganglioside biosynthesis and prevent oncogenic transformation (Bremer et al., 1984; Hakomori, 1981). Gangliosides are

† This work was supported by Deutsche Forschungsgemeinschaft Grants Ga 233/10, Schw 143/5-3, and Sa 257/11-5.
‡ Technische Hochschule Darmstadt.
§ Universität Bonn.

0006-2960/87/0426-5943$01.50/0

receptors for viruses, bacterial toxins, and hormones. G_{M1} is a specific receptor for cholera toxin (Goins & Freire, 1985; Spiegel, 1985), G_{D1b} and G_{T1b} mediate the binding and translocation of tetanus toxin into the cell (Lazarovici & Yavin, 1985). There are other nonphysiologically occurring gangliosides, e.g., G_{M2}, which accumulates in gangliosidosis patients having an enzyme or activator (hexosaminidase A) defect (Conzelmann & Sandhoff, 1978). Gangliosides are believed to modulate the immune response of the cell and the binding of antibodies to neighboring membrane components (Shichijo & Alving, 1986). In these processes gangliosides give a specific contribution to the structural stability and recognition of the membrane. This contribution is evidently dependent upon their chemical and physicochemical properties.

Due to their amphipathic character, gangliosides tend to aggregate in water, forming high molecular weight micelles (Yohe & Rosenberg, 1972; Yohe et al., 1976; Formisano et al., 1979; Mraz et al., 1980). Most values for their critical micelle concentrations found in the literature are in the range of 10^{-4}–10^{-6} M (Gammack, 1963; Yohe & Rosenberg, 1972; Yohe et al., 1976; Corti et al., 1980), whereas Formisano et al. (1979) and Mraz et al. (1980) found a value which is much lower (10^{-8}–10^{-10} M). This striking discrepancy demonstrates the need for further evaluation. In this study we used a fluorescence method, the excimer-formation technique, for the investigation of ganglioside association.

In cerebral gray matter gangliosides are particularly abundant. They comprise up to 10–15% of total lipid in synaptosomal membrane fractions. Rahmann and Hilbig (1983) reported that gangliosides are involved in synaptic transmission and memory formation and show a pronounced ability to complex with Ca^{2+}, leading to altered membrane permeability. Hayashi et al. (1984) observed increased Ca^{2+} binding with increasing sialic acid content in a chelate-like form. The ability of Ca^{2+} to phase separate gangliosides in phospholipid membranes has also been reported by the use of fluorescence and calorimetric (DSC) studies (Goins & Freire, 1985; Masserini & Freire, 1986). Masserini and Freire (1986) found ganglioside phase separation induced by 5 mM Ca^{2+}, but it remained questionable whether this was a Ca^{2+} effect on ganglioside or on the phospholipid matrix. Other laboratories, using different methods, found very little Ca^{2+}-binding affinity of gangliosides and complete miscibility between gangliosides and phospholipids in the presence of Ca^{2+} (Sela & Bach, 1984; McDaniel & McLaughlin, 1985; Maggio et al., 1980).

Ganglioside distribution in a phospholipid environment, the affinity for Ca^{2+}, and phase-separation phenomena are not well understood. Evidence for distributional differences between different ganglioside species in phospholipid model membranes was monitored by electron microscopy (Peters et al., 1984). G_{M1} distributes preferentially in $P_{\beta'}$ ripples whereas G_{D1a} does not show such a preference. On the contrary, Thompson et al. (1985) reported that G_{M1} is uniformly distributed rather than being clustered in undispersed patches.

In this study we are dealing with the properties of gangliosides in aqueous solution and in phosphatidylcholine model membranes. Using pyrene-labeled gangliosides, the label being situated at the end of their fatty acid regions, and the excimer technique, we studied micellization, lateral diffusion, and distribution in the presence and absence of Ca^{2+}. These fluorescence-labeled lipids are useful probes for the study of the physical and structural properties of lipid bilayer membranes.

The excimer-formation technique is based on the ability of pyrene derivatives to form excited dimers (excimers) between ground state and excited molecules (Förster, 1969). The excimer shows a distinct emission at a longer wavelength than the excited monomer. In an isotropic solution (Birks et al., 1963) or in a lipid bilayer membrane (Galla & Sackmann, 1974), it is possible to determine the association constant of the excimer formation. The latter is related to the self-diffusion coefficient or the average jump frequency of the lipid molecules within the lipid matrix (Galla et al., 1979). A requisite for the calculation of the diffusion coefficient is a homogeneous probe concentration, thus assuming a linear concentration dependence of the excimer-to-monomer fluorescence intensity ratio. Nonlinear concentration dependence is an indication for phase-separation phenomena (Galla & Sackmann, 1975).

Since the early work of Galla and Sackmann (1974), pyrene-labeled lipids have been in widespread use as a means to investigate the mechanism of lateral diffusion (Müller et al., 1986), phospholipid lateral phase separation (Somerharju et al., 1985; Wiener et al., 1985), and also interbilayer lipid transfer (Galla et al., 1979; Wong et al., 1984). Hresko et al. (1986) published a study of the lateral distribution of pyrene-labeled phosphatidylcholine in PC[1] bilayers. The shape of the phase-transition curves, obtained from the temperature dependence of the excimer-to-monomer intensity ratio, provides information on the probe distribution. A clear distinction between ideal and nonideal mixing behavior of different types of lipids can be made.

Materials and Methods

Lipids and Fluorescent Probes. 1,2-Dimyristoyl- and 1,2-dipalmitoyl-*sn*-glycero-3-phosphocholines (DMPC and DPPC), obtained from Fluka (Neu Ulm, FRG), were checked by thin-layer chromatography and used without further purification. Pyrene-labeled phosphatidylcholine was synthesized according to the method of Galla and Hartmann (1981) and was kindly provided by J. Becker. Calcium chloride dihydrate (grade I) was obtained from Sigma (München, FRG). 12-(1-Pyrenyl)dodecanoic acid was obtained from Molecular Probes (Junction City, OR). *N*,*N*-Dicyclohexylcarbodiimide (DCC), *N*-hydroxysuccinimide, and diisopropylethylamine were purchased from Fluka (Buchs, Switzerland). Silica gel LiChroprep Si100 (25–40 μm), precoated thin-layer plates Kieselgel 60 (0.25-mm layer thickness), and analytical grade solvents were from E. Merck (Darmstadt, FRG).

Ganglioside Extraction. Gangliosides [nomenclature according to Svennerholm (1963)] were extracted from bovine brain with mixtures of chloroform/methanol/0.1% potassium chloride and partitioned as described by Folch et al. (1957), prior to separation on DEAE-Sephadex A-25 (Ledeen & Yu, 1982; Momoi et al., 1976). Final purification of gangliosides G_{M1}, G_{D1a}, and G_{D1b} was achieved by medium-pressure column chromatography (1.2 × 100 cm) on LiChroprep Si100, using

[1] Abbreviations: DPPC, 1,2-dipalmitoyl-*sn*-glycero-3-phosphocholine; DMPC, 1,2-dimyristoyl-*sn*-glycero-3-phosphocholine; PyC_{10}, 10-(1-pyrenyl)decanoic acid; PyPC, 1-acyl-2-[10-(1-pyrenyl)decanoyl]-*sn*-glycero-3-phosphocholine; PyG_{M3}, *N*-[12-(1-pyrenyl)dodecanoyl]-lyso-G_{M3}; PyG_{M2}, *N*-[12-(1-pyrenyl)dodecanoyl]-lyso-G_{M2}; PyG_{M1}, *N*-[12-(1-pyrenyl)dodecanoyl]-lyso-G_{M1}; PyG_{D1a}, *N*-[12-(1-pyrenyl)dodecanoyl]-lyso-G_{D1a}; PyG_{D1b}, *N*-[12-(1-pyrenyl)dodecanoyl]-lyso-G_{D1b}; T_t, main phase transition temperature; cmc, critical micelle concentration; PC, phosphatidylcholine; DMF, *N*,*N*-dimethylformamide; Tris, tris(hydroxymethyl)aminomethane; I_M, fluorescence intensity of the monomeric pyrene probe; I_D, fluorescence intensity of the excimer; TLC, thin-layer chromatography.

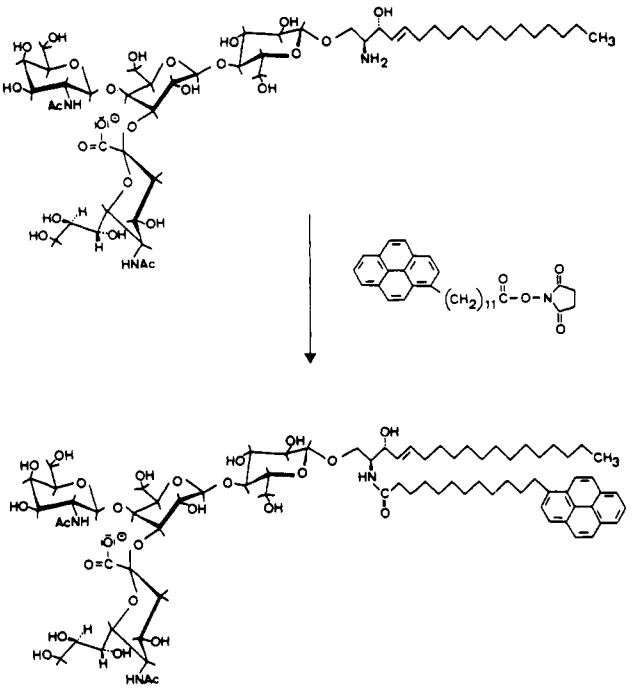

FIGURE 1: Reaction scheme for synthesis of pyrene-labeled ganglioside PyG_{M2}. Pyrenyldodecanoic acid was covalently attached to the ceramide moiety. The length of the fatty acid chain was chosen to obtain a good fit with the dye molecule.

mixtures of chloroform/methanol/water of increasing polarity or linear gradients of 2-propanol/*n*-hexane/water (55/45/5 to 55/25/15 v/v/v). Gangliosides G_{M2} was isolated from the post-mortem brain of a Tay–Sachs patient and purified as described by Svennerholm (1972). Ganglioside G_{M3} was prepared from post-mortem human spleen as described (Schwarzmann, 1978).

Preparation of 12-(1-Pyrenyl)dodecanoate N-Succinimidyl Ester. *N*-Succinimidyl pyrenyldodecanoate was prepared as described for fatty acid *N*-succinimidyl ester by Lapidot et al. (1967). Briefly, 12-(1-pyrenyl)dodecanoic acid (50 μmol) was dissolved in dry ethyl acetate (1 mL) and mixed with an equimolar amount of solid *N*-hydroxysuccinimide. After the latter had dissolved, an equimolar amount of solid *N*,*N*-dicyclohexylcarbodiimide was added and the mixture was stirred under argon overnight at 25 °C. *N*,*N*-Dicyclohexylurea was removed by centrifugation and the clear supernatant dried in a nitrogen jet. The dry residue was then dissolved in anhydrous *N*,*N*-dimethylformamide (DMF; 0.5 mM) and stored under argon at −20 °C until use.

Thin-Layer Chromatography. The purity of compounds during reaction courses and column chromatographic elution profiles was routinely checked by thin-layer chromatography (TLC). Gangliosides and pyrene-labeled gangliosides [*N*-[12-(1-pyrenyl)dodecanoyl]lysogangliosides] were developed in chloroform/methanol/15 mM calcium chloride (60/35/8 v/v/v) for monosialogangliosides and their pyrene-labeled derivatives or (60/40/9 v/v/v) for disialogangliosides and their pyrene-labeled derivatives.

Synthesis of Pyrene-Labeled Gangliosides. Pyrene-labeled gangliosides PyG_{M3}, PyG_{M2}, PyG_{M1}, PyG_{D1a}, and PyG_{D1b} were synthesized as described by Schwarzmann and Sandhoff (1987) and Neuenhofer et al. (1985), starting from the appropriate lysogangliosides. The reaction scheme is shown in Figure 1. Briefly, a solution of lysoganglioside (5 μmol) in DMF (0.4 mL) and diisopropylethylamine (20 μL) was mixed with *N*-succinimidyl pyrenyldodecanoate (10 μmol) in DMF (0.1 mL) and stirred under argon at 30 °C for 2 days in the dark. Subsequently, the solvents were removed in a nitrogen jet, and the residue was purified by column chromatography on LiChroprep Si100 (0.6 × 90 cm) with a linear gradient of 2-propanol/*n*-hexane/water (55/40/5 v/v/v and 55/25/15 v/v/v, respectively) for pyrene-labeled monosialo- and disialogangliosides. Values on TLC were determined by visualizing the spots with both UV light (366 nm) and spraying with anisaldehyde reagent followed by heating (Stahl & Kaltenbach, 1961). All of these pyrene-labeled gangliosides exhibit slightly higher R_f values than their parent gangliosides. Quantification of pyrene-labeled gangliosides was performed by the determination of sialic acid content and weight. The yield of the purified compounds was generally 4 μmol (80%) with respect to the lysogangliosides. The used lyso-G_{M3} was homogeneous in chain length ($C_{18:1}$) whereas the other species were mixtures of $C_{18:1}/C_{20:1}$ in a long-chain base. However, the thermotropic behavior of gangliosides is not influenced by these chain-length differences (Masserini & Freire, 1986).

Preparation of Micellar Dispersions. Pyrene-labeled lipids were dried from a solution in chloroform/methanol (1:1 v/v) at 45 °C by a stream of nitrogen. Lipid films were kept in a vacuum oven for at least 2 h at 45 °C. Dispersions were prepared in 10 mM Tris-HCl buffer (pH 7.2) by short sonication (Branson sonifier B15, microtip, power level 20 W), starting from high to low concentration. Each dilution step in the course of cmc determination was accompanied by a short sonication at 25 °C followed by a 10-min equilibration of the probe before measurement.

Vesicle Preparation. DMPC and DPPC vesicles containing pyrene-labeled lipids were prepared by moderate sonication. Lipids were dissolved in chloroform/methanol (1:1 v/v). The solvent was removed at 50 °C by a stream of nitrogen and by subsequent evaporation in a vacuum oven for 2 h at 50 °C. 10 mM Tris-HCl buffer (pH 7.2) was added to make up a final lipid concentration of 1 mg/mL, and the samples were sonicated for 3 min at 50 °C (Branson sonifier B15, microtip, 20 W). Vesicle dispersions were held at 21 °C for several hours before fluorescence measurement. Each sample was measured in the absence and in the presence of Ca^{2+}. A 1 M stock solution of $CaCl_2$ was the source of the latter. Samples were kept at 21 °C for at least 6 h after Ca^{2+} addition. The consequent dilution of the lipid dispersion after the addition of Ca^{2+} solution did not effect the excimer-to-monomer fluorescence intensity ratio. The excimer yield depends on the concentration of labeled lipid within the membrane but not on that of total lipid in the aqueous phase.

Analytical Methods. The amount of ganglioside incorporated into DPPC vesicles in the course of sample preparation and the amount of ganglioside-bound sialic acid during pyrene-labeled ganglioside synthesis were determined according to the resorcinol method of Svennerholm (1957). Vesicles used for spectroscopic measurements were sedimented in the presence of 200 mM Ca^{2+} by 3 h of centrifugation at 12500*g* (Hettich microcentrifuge). The ganglioside content was quantified in the sediment and in the supernatant. Pure *N*-acetylneurominic acid (Serva, Heidelberg, FRG) was used as a standard. The phospholipid content of the mixed phospholipid/ganglioside vesicles was determined from phosphate analysis according to the method of Chen et al. (1956). Pure sodium dihydrogenphosphate (Fluka, Neu Ulm, FRG) was used as a standard. The sediment and supernatant of the centrifuged probes was handled separately in that way. The amount of ganglioside and phospholipid present in the mixed vesicles was recalculated from the analytical data.

Spectroscopic Method and the Excimer-Formation Technique. Fluorescence measurements were performed with a Perkin-Elmer MPF-3 spectrometer. Samples were kept in a 0.5-cm quartz cuvette in a thermostated metal block. Temperature was controlled by a thermocouple in the sample with a Keithley digital thermometer. Pyrene lipids were excited at λ = 340 nm. For each heating step, the monomer and excimer emission (I_M and I_D, respectively) were calculated from the corresponding monomer peak at λ = 395 nm and the broad excimer band at λ = 470 nm.

For determination of the micellar properties of the pyrene-labeled lipids, the monomer fluorescence intensity was measured at λ = 365 nm. In these experiments the monomer band intensity is considerably impinged upon by that of the excimer band. However, the masking effect of the latter is not so pronounced if the lower wavelength monomer band is used for measurements. All spectra were taken at 25 °C. The excitation slit was held minimal to exclude bleaching of the probe.

The diffusion coefficients can be determined from the fluorescence intensities of the excimer I_D and the monomer I_M of pyrene molecules incorporated into the membrane. The intensity ratio I_D/I_M is a measure for the diffusion-controlled collision process of pyrene molecules incorporated into lipid bilayer membranes. The jump frequency ν_j in a lipid matrix is directly related to the excimer lifetime, which has to be measured separately. In our experiments τ_D was 70 ± 10 ns for all probes at 45 °C. The coefficient of the lateral diffusion D_{diff} is related to the jump frequency, ν_j, by $D_{diff} = {}^1/_4\ \nu_j\lambda^2$. The term is the length of one diffusional step as given by the average distance of two neighboring lipid molecules (λ = 0.8 nm). In this paper the translational diffusion is characterized by the diffusion coefficient. For further details see the papers by Galla and Hartmann (1980) and Galla et al. (1979).

Results

Micelle Formation of Pyrene-Labeled Gangliosides. Pyrene derivatives form excimers, if excited and ground-state monomer molecules contact within the lifetime of the excited monomer. This may occur by a diffusion-controlled process or by the formation of domains in mixtures or aggregates of the pyrene-labeled species in solution (Galla & Hartmann, 1980; Galla et al., 1979). Here we used the excimer formation technique to investigate the process of ganglioside aggregation formation.

Typical fluorescence spectra of pyrene-labeled G_{M1} in a low range of concentrations, in aqueous solution, are given in Figure 2. From these spectra we obtain at 2×10^{-8} M concentration a fluorescence intensity ratio, I_D/I_M, measured at λ = 365 and 470 nm for the monomer and excimer emission, respectively, of $I_D/I_M = 1.43$. At $c = 1.4 \times 10^{-7}$ M it increases to $I_D/I_M = 3.9$, and at a concentration of 6.3×10^{-7} M the excimer band exceeds the monomer band more than 5-fold. This height of the I_D/I_M ratios clearly shows that PyG_{M1} attends a micellar rather than a monomeric form.

In Figure 3 the concentration dependence of the excimer-to-monomer intensity ratio is given for PyG_{M1}, PyG_{M3}, and PyG_{D1a} in comparison to PyPC. Below 10^{-7} M the I_D/I_M value increases in the order PyPC < PyG_{M3} < PyG_{M1} < PyG_{D1a}. Between 10^{-7} and 10^{-6} M the I_D/I_M value obtained for PyG_{M3} exceeds the one for PyG_{M1}. At concentrations above 10^{-6} M the I_D/I_M vs. concentration curve of PyG_{D1a} has a smaller slope compared to the other lipids used and therefore crosses the other curves. PyG_{M3} and PyG_{M1} exhibit a maximal excimer-to-monomer ratio of about 55 at 10^{-5} M, whereas it is about half the value for PyG_{D1a} at that concentration.

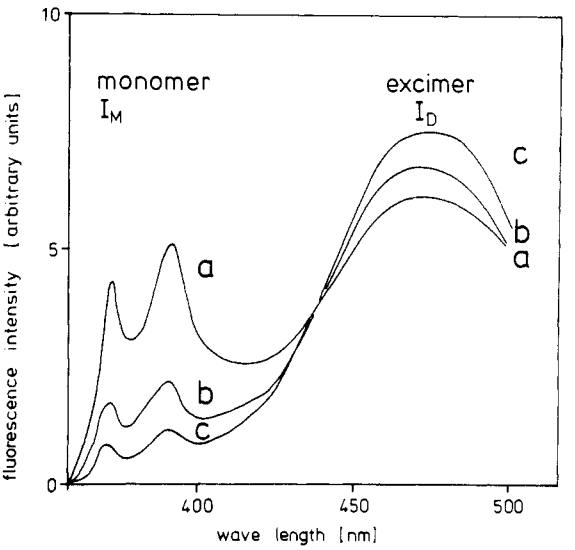

FIGURE 2: Fluorescence spectra of PyG_{M1} in aqueous suspension at three different concentrations. Probes were sonicated in buffer and incubated at 25 °C for 10 min before measurement. The excitation wavelength was at 340 nm. The excimer peak at 470 nm and the monomer peak at 365 nm were taken to calculate the I_D/I_M fluorescence intensity ratio. Spectrum a: the probe concentration was 2×10^{-8} M with an I_D/I_M value of 1.4. Spectrum b: the probe concentration was 1.4×10^{-7} M with an I_D/I_M value of 3.9. Spectrum c: the probe concentration was 6.3×10^{-7} M with an I_D/I_M value of 8.9.

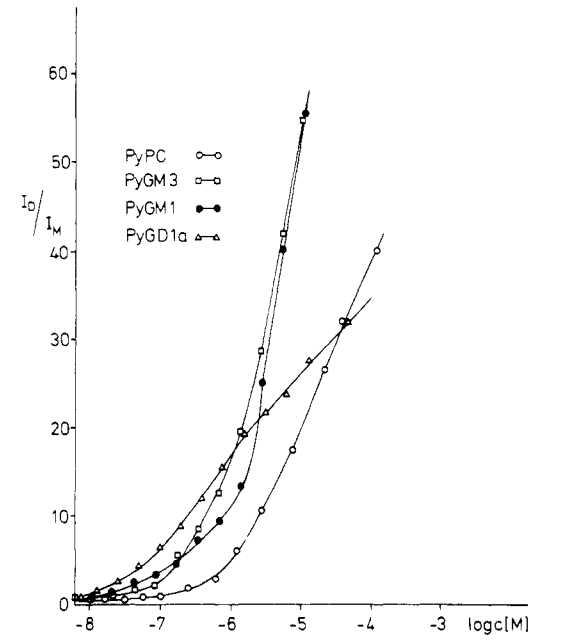

FIGURE 3: Excimer-to-monomer intensity ratio (I_D/I_M) is given as function of concentration (log c) for PyPC (○), PyG_{M3} (□), PyG_{M1} (●), and PyG_{D1a} (△). Each value was taken from the corresponding spectrum as shown in Figure 2. Samples were prepared by stepwise dilution in 10 mM Tris-HCl buffer, pH 7.2. Each dilution step was followed by a short sonication at 25 °C. Excitation and emission wavelengths were as in Figure 2.

Concentration Dependence of the Excimer Formation and Lateral Diffusion. Pyrene-labeled gangliosides were incorporated into dipalmitoylphosphatidylcholine (DPPC) bilayer membranes in a molar ratio between 2 and 8 mol % with respect to total lipid. From the fluorescence spectra we determined the I_D/I_M values with probe concentration at T = 45 °C, which is above the main phase transition temperature of the host lipid. Results are summarized in Figure 4. I_D/I_M values obtained with pyrenyldecanoic acid and pyrene-labeled

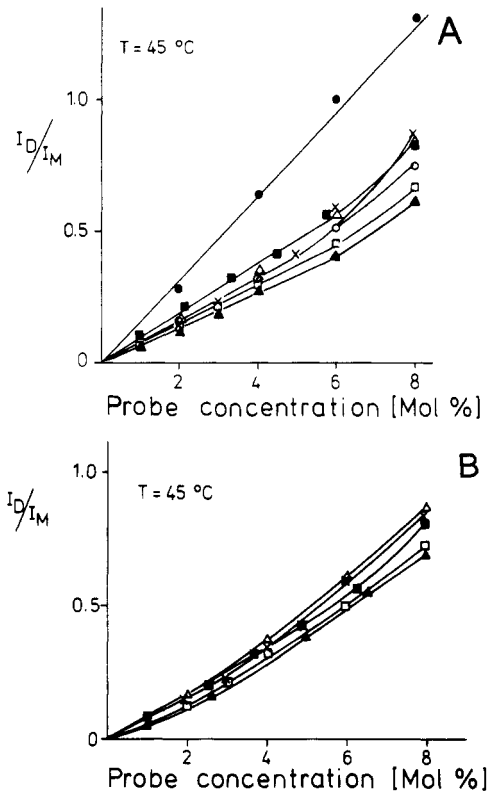

FIGURE 4: (A) The excimer-to-monomer fluorescence intensity ratio, I_D/I_M, calculated from peak maxima from corresponding spectra is given as function of probe concentration in small unilamellar DPPC vesicles at 45 °C. Mixed vesicles were obtained by cosonication of DPPC and the corresponding pyrene-labeled lipid at a total lipid concentration of 1 mg/mL. From the linear part of the curves taken at 45 °C it was possible to calculate the diffusion coefficients in the fluid membranes. Symbols used for the different pyrene-labeled probes are ●, PyC_{10}; ○, PyPC; ■, PyG_{M3}; ×, PyG_{M2}; △, PyG_{M1}; ▲, PyG_{D1a}; □, PyG_{D1b}. (B) Same as (A) but in the presence of 200 mM Ca^{2+}. Spectra were taken after equilibration of the Ca^{2+}-containing probes for a minimum of 6 h.

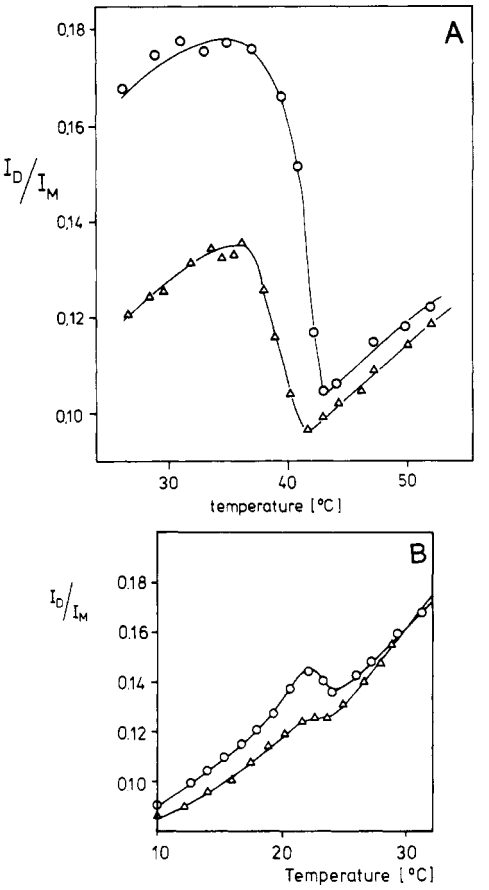

FIGURE 5: (A) Thermotropic phase transition curves of DPPC vesicles containing 2 mol % PyPC as fluorescent probe in the absence of Ca^{2+} (△) and in the presence of 200 mM Ca^{2+} (○). The excimer-to-monomer fluorescence intensity ratio, I_D/I_M, was calculated from the corresponding fluorescence spectra for each temperature. (B) Thermotropic phase transition curves of DMPC vesicles containing 2 mol % PyPC. Curves were taken in the absence of Ca^{2+} (△) and in the presence of 200 mM Ca^{2+} (○).

phosphatidylcholine are given for comparison.

The concentration dependence of the I_D/I_M ratio is linear up to 6 mol % for all probes but shows a slight upward bend above 6 mol %. The diffusion coefficients of gangliosides in the fluid DPPC membranes can be calculated from the slopes of the initial straight lines. The diffusion of PyPC is characterized by $D_{diff} = 1.6 \times 10^{-7}$ cm^2/s. Considering the error of determination, this correlates satisfactorily with values for all pyrene-labeled monosialogangliosides. For disialogangliosides, however, the D_{diff} is slightly reduced in DPPC membranes.

At a given probe concentration the addition of Ca^{2+} in a 200 mM concentration causes a small but visible deviation from a straight concentration dependence (Figure 4B). An upward deflection of the I_D/I_M values occurs already at low probe concentrations. However, the observed effect is extremely small compared to a complete phase separation as could be induced in phosphatidic acid containing PC membranes (Galla & Sackmann, 1975). Thus this result supports an interpretation that Ca^{2+} does not induce significant changes in the lateral organization of gangliosides in PC membranes.

Thermotropic Phase Transition Curves. Very recently Hresko et al. (1986) published simulated I_D/I_M vs. temperature curves that allow the interpretation of phase transition curves obtained by the excimer technique. From the shape of the temperature dependence of the I_D/I_M ratio, it is possible to obtain information on the lateral distribution of pyrene probes within a lipid bilayer.

Figure 5A gives an example for a phase-transition curve of a completely miscible probe with nonideal mixing behavior. The experimental values were obtained with PyPC in DPPC membranes in both the absence and presence of Ca^{2+}. In the gel and fluid phases the I_D/I_M ratio increases with temperature, whereas in the phase-transition region it decreases. At $T > T_t$ the I_D/I_M ratio increases linearly with temperature, and thus diffusion coefficients may be calculated in this range. According to Hresko et al. (1986) the height of the I_D/I_M peak between 30 and 40 °C is a measure of the probe's preference for a fluid state.

Figure 5B shows a similar experiment, but DMPC was used instead of DPPC. In the absence of Ca^{2+}, the I_D/I_M vs. temperature curve only exhibits a discontinuity instead of the sharp decrease with increasing temperature at T_t. This is characteristic for a homogeneous probe distribution with nearly ideal mixing.

Addition of Ca^{2+} induces a drastic increase of the peak height in DPPC membranes, whereas in DMPC membranes, the peak becomes visible but remains small. Note that the lipid phase transition temperature is increased by about 2 °C in the presence of 200 mM Ca^{2+} and that the change in the I_D/I_M ratio is negligible in the fluid phase.

Another group of experiments was performed with pyrene-labeled gangliosides as probe molecules. Figure 6 gives the phase-transition curves of DPPC membranes obtained with different concentrations of PyG_{M3} in the absence and presence of Ca^{2+}. In the absence of Ca^{2+} the host lipid phase transition

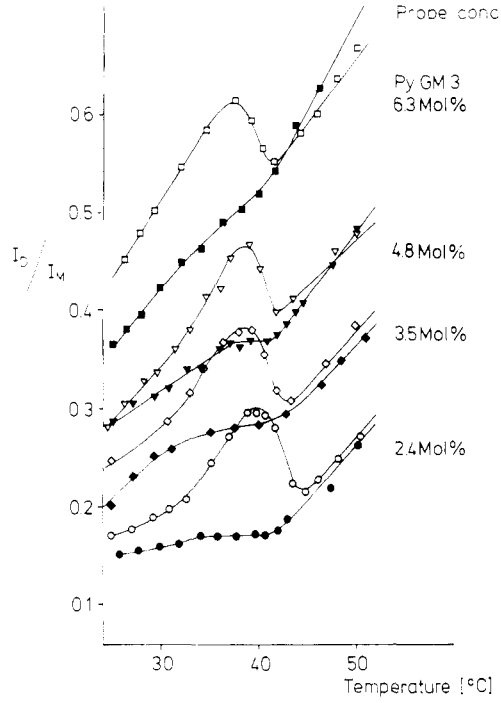

FIGURE 6: Thermotropic phase transition curves of DPPC vesicles obtained by the excimer-formation technique. PyG_{M3} was used as probe molecule at 2.4–8 mol % concentration with respect to DPPC. Lipid and ganglioside were cosonicated at a final concentration of 1 mg/mL in 10 mM Tris, HCl buffer, pH 7.2. Closed symbols were chosen for the phase-transition curves in the absence of Ca^{2+}. Open symbols were used for the phase-transition curves in the presence of 200 mM Ca^{2+}. Probes containing Ca^{2+} were equilibrated for at least 6 h before measurement. Samples were excited at 340 nm; I_D/I_M values were calculated from the fluorescence spectra at the appropriate temperature.

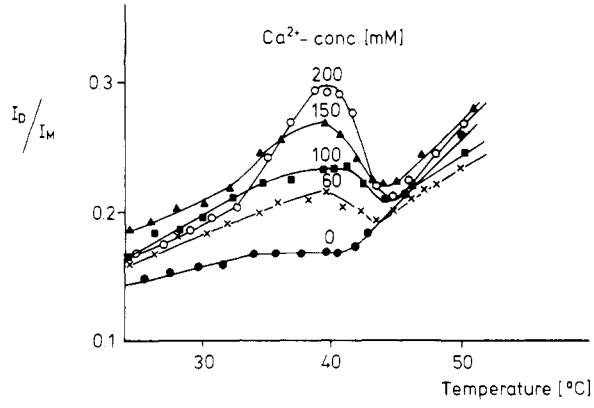

FIGURE 7: Influence of Ca^{2+} on the thermotropic phase transition of DPPC vesicles containing 4 mol % PyG_{M3} as probe molecule. The experimental procedure is the same as that described in Figure 6.

is signified by a plateau in the temperature curve. This is best documented at 2.4, 3.5, and 4.8 mol %. The curves resemble that of PyPC in DMPC membranes, but the plateau just below the phase-transition temperature covers a broader temperature range. At higher PyG_{M3} concentrations (e.g., 6.3 and 8 mol %), the plateau between 36 and 41 °C disappears, and the transition curve exhibits subsequently a continuous increase of the I_D/I_M values with temperature.

Addition of 200 mM Ca^{2+} leads to the appearance of an I_D/I_M peak comparable to the one observed with PyPC in DPPC membranes (Figure 5A). The emerging of the peak induced by increasing Ca^{2+} concentration is shown in Figure 7. At 60 mM Ca^{2+} the peak starts to develop and reaches the final value at about 200 mM. Higher concentrations do not induce further effects. Note that the Ca^{2+} effect is most pronounced at PyG_{M3} concentrations between 2 and 5 mol %.

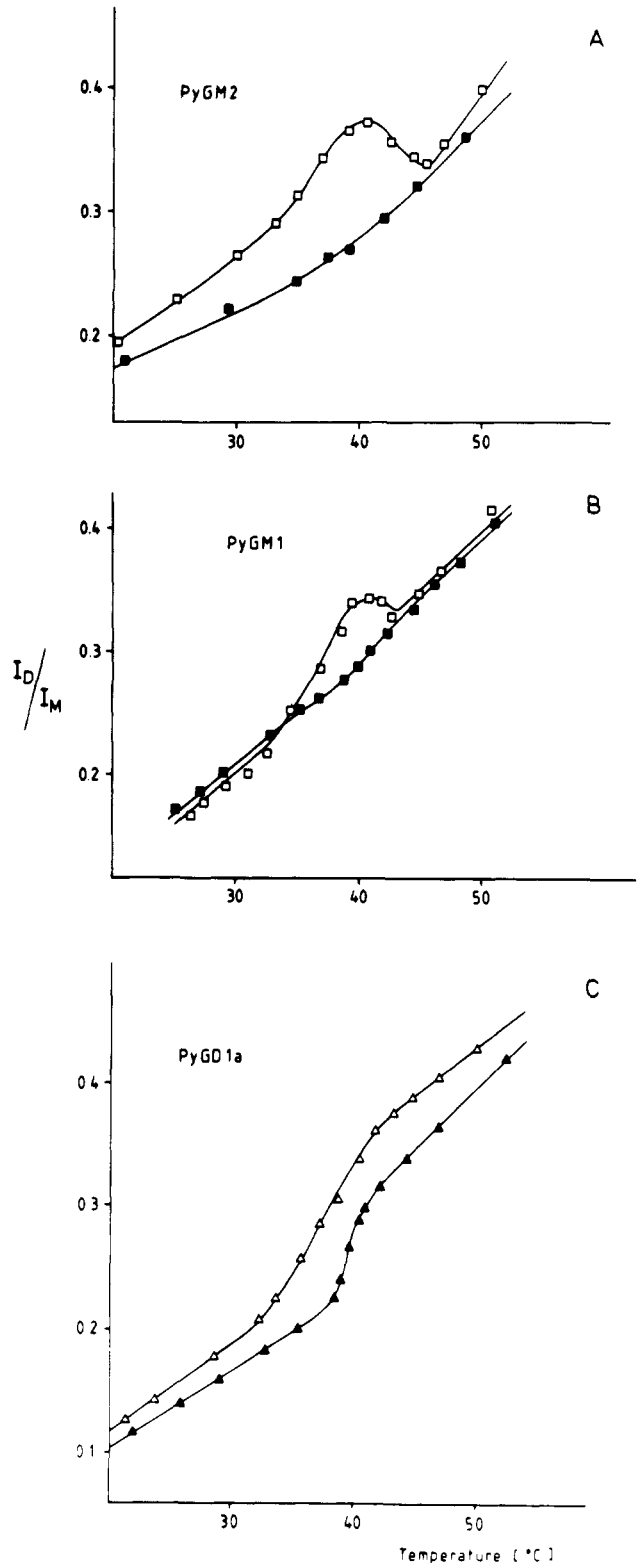

FIGURE 8: Thermotropic phase transition of DPPC vesicles containing the following pyrene-labeled ganglioside concentrations: (A) 4 mol % PyG_{M2}; (B) 4 mol % PyG_{M1}; (C) 5 mol % PyG_{D1a}. Closed symbols give the phase-transition curves without Ca^{2+}, and open symbols are used for probes containing 200 mM Ca^{2+}. The experimental procedure is the same as that described in Figure 6.

Similar experiments were performed with PyG_{M2}, PyG_{M1}, and PyG_{D1a} (panels A, B, and C of Figure 8, respectively). With PyG_{M2} as probe molecule and in the absence of Ca^{2+}, the phase-transition curves of the DPPC host membrane did

not show the plateau obtained with PyG_{M3}. Only a discontinuity was observed at T_t. Remarkably, in the presence of 200 mM Ca^{2+} the emergence of the I_D/I_M peak below the phase-transition temperature is observed. The effect is most pronounced in a low probe concentration range, between 2 and 4 mol %.

With PyG_{M1} the discontinuity at the phase transition is even less pronounced compared to that of PyG_{M2}. In the presence of 200 mM Ca^{2+} the peak around 40 °C is smaller compared to that for PyG_{M2} and much smaller compared to that for PyG_{M3}.

A further change in the shape of the phase-transition curves was obtained with PyG_{D1a}. The phase transition is now marked by an increase in the I_D/I_M ratio, most clearly visible at 5 mol % PyG_{D1a}. This shape for a phase-transition curve is typical for a probe with ideal mixing behavior. Ca^{2+} ions do not induce the reappearance of a peak. This experiment clearly indicates that PyG_{D1a} distributes randomly and mixes ideally in DPPC membranes, even in the presence of high amounts of Ca^{2+}. With PyG_{D1b} as the probe molecule we obtained an effect similar to that with PyG_{D1a} (data not shown).

Effect of Ca^{2+}. Phase-transition curves shown so far, in the presence of Ca^{2+}, were taken after at least 6 h of incubation with Ca^{2+}. However, the Ca^{2+} effect is time dependent. Figure 9 summarizes the short- and long-time Ca^{2+} effects. A DPPC sample containing 4 mol % PyG_{M3} is shown as an example. In Figure 9A a typical phase-transition curve is shown in the absence of Ca^{2+} (●) and in the presence of 200 mM Ca^{2+} after incubation for 8 h at 38 °C (○). A third curve (□) shows the immediate effect following Ca^{2+} addition. The I_D/I_M peak below the phase transition is less pronounced and does not change even on the addition of Ca^{2+} up to 200 mM or if the phase-transition curve is measured immediately.

This is demonstrated in Figure 9B, showing the immediate response of the I_D/I_M value to Ca^{2+} at 38 °C. Up to 100 mM Ca^{2+} the response amplitude increases with increasing Ca^{2+} concentration. Higher Ca^{2+} concentrations do not further increase the immediate response. However, the increase in the I_D/I_M ratio continues with time if the Ca^{2+} concentration exceeds 100 mM. The final value depends on the Ca^{2+} concentration. As shown in Figure 9C, Ca^{2+} in 100 or 200 mM concentration induces the same initial increase in the I_D/I_M value measured at 38 °C. At 100 mM Ca^{2+} the final peak height is reached immediately. If Ca^{2+} is subsequently added to make 200 mM, the immediate response is the same; however, the increase in peak height, shown in Figure 9A, proceeds slowly and reaches a constant value after 8–10 h.

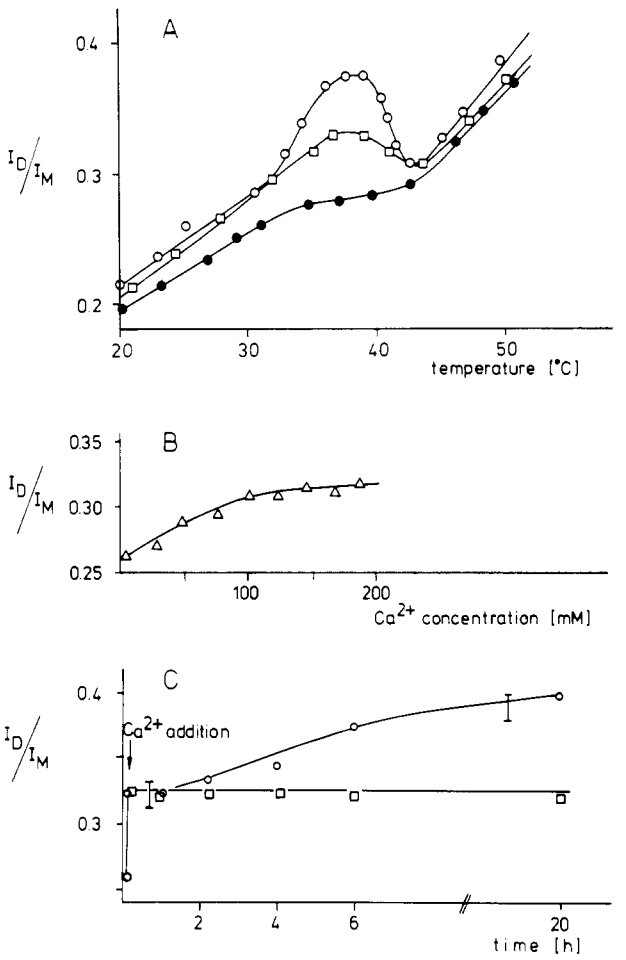

FIGURE 9: Temperature, concentration, and time dependence of the Ca^{2+} effect on DPPC vesicles containing 4 mol % PyG_{M3}. In panel A thermotropic phase transition curves are shown in the absence of Ca^{2+} (●), with 100 mM Ca^{2+} (□), and with 200 mM Ca^{2+} (○). The phase-transition curve obtained with 100 mM Ca^{2+} remains the same immediately after Ca^{2+} addition and after several hours of incubation. This shape is also obtained with 200 mM Ca^{2+} measured directly after Ca^{2+} addition. However, an increase in the I_D/I_M peak height around 38 °C occurs with time. Curve (○) was recorded after 8 h of incubation in the presence of 200 mM Ca^{2+}. Panel B: the I_D/I_M ratio of DPPC–4 mol % PyG_{M3} was taken as function of Ca^{2+} concentration in a titration experiment at 38 °C. Spectra were measured immediately after Ca^{2+} addition. Panel C: the time dependence of the I_D/I_M ratio for DPPC vesicles containing 4 mol % PyG_{M3} at 100 mM Ca^{2+} (□) and 200 mM Ca^{2+} concentration (○). Probes were held at 38 °C in the cuvette during the experiment. Irradiation of the probe was only performed during recording of the spectra to avoid bleaching.

Discussion

The micelle formation of different gangliosides has been studied by a variety of techniques for many years. Early values of the critical micelle concentration (cmc) were reported to be around 10^{-4}–10^{-5} M (Trams & Lauter, 1962; Gammack, 1963; Yohe & Rosenberg, 1972; Yohe et al., 1976). However, more recent investigations report micellization occurring at extremely lower concentrations around 10^{-9}–10^{-10} M (Mraz et al., 1980; Formisano et al., 1979). From laser light scattering data Corti et al. (1980) derived an upper limit for the cmc of 10^{-6} M, and the hydrodynamic radius of the micelles was found to depend on sialic acid content.

Using fluorescence spectroscopy, we investigated the micellar properties of pyrene-labeled gangliosides in the concentration range of 10^{-4}–10^{-8}M as shown in Figure 2. Basically, excimers are formed if pyrene molecules are already in close contact before excitation or if the dimerizations occur via collision in a diffusion-controlled process during the lifetime of the excited monomer. However, excimer formation in solution due to collision occurs only at concentrations larger than 10^{-4} M (Förster, 1969). The fluorescence spectra of pyrene-labeled gangliosides in an organic solvent at low concentration exhibit an intensity ratio, I_D/I_M, as low as 0.03. Therefore, such a diffusion-controlled excimer formation can be excluded in the concentration range under investigation. From the I_D/I_M vs. concentration curves in Figure 3, we find that the I_D/I_M values at 2×10^{-8} M concentration is 0.9, 1.3, and 1.4 for PyG_{M3}, PyG_{M1}, and PyG_{D1a}, respectively. These values are considerably higher than the value obtained for an isotropic solution ($I_D/I_M = 0.03$). The latter value gives the minimum I_D/I_M value if no excimer formation occurs and the intensity at $\lambda = 470$ nm is only determined by the long-wavelength tail of the monomer emission (spectra not shown). Therefore, our data present strong evidence for the existence of micelles at ganglioside concentrations above 2×10^{-8} M, which is the upper limit of the cmc observable with our

fluorescence equipment. Below 10^{-7} M the excimer yield increases successively from PyPC to PyG_{D1a} as outlined above. Obviously the highest tendency for an association is correlated with a higher degree of sialylation and with a larger oligosaccharide part.

The I_D/I_M values for PyG_{M1} and PyG_{M3} increase smoothly over a concentration range from 10^{-8} to 10^{-7} M and more steeply from $c = 10^{-7}$ M to higher concentrations. The curve for PyG_{D1a} which is identical with the curve obtained with PyG_{D1b} (not shown) starts at a higher I_D/I_M value at low PyG_{D1a} concentration but increases very smoothly up to $I_D/I_M = 30$ at 3×10^{-5} M. This is a remarkable fact since it gives information about the homogeneity of the micelle population. Our data shown in Figure 3 are only explainable if we assume a coexistence of numerous micellar aggregates differing in size and shape. PyG_{D1a}, which has the highest I_D/I_M value at low concentration, shows the lowest value at high concentrations. We assume that above 10^{-6} M concentration PyG_{D1a} or PyG_{D1b} form smaller micelles than PyG_{M3} or PyG_{M1}. This is in agreement with the light scattering data of Corti et al. (1980), who reported an aggregation number of 352 and 229 molecules per micelle for G_{M1} and G_{D1a}, respectively. Ganglioside G_{D1a}, with the highly sialylated space-filling head group, is thought to form an average of smaller micellar aggregates that have a higher curvature. In such a configuration a splay deformation may occur that prevents the pyrene molecules attached to the ceramide fatty acid chains from aligning parallel to each other, a requirement that is necessary for an efficient excimer formation. The larger G_{M1} or G_{M3} micelles allow a better parallel orientation of the ceramide chains due to the smaller ratio of the space occupied by the head group and the ceramide part.

So far we have discussed the micellar behavior of pyrene-labeled gangliosides in aqueous solution. The next set of experiments were concerned with pyrene-labeled gangliosides in DPPC membranes. The first thing to notice is the change in the relative intensities of the structured monomer emission. In ganglioside micelles the first monomer peak at $\lambda = 365$ nm was smaller than the second one at $\lambda = 395$ nm (Figure 2). In DPPC membranes the situation is reversed due to the more apolar surrounding of the pyrene residue. In the concentration range between 2 and 8 mol % pyrene-labeled ganglioside with respect to DPPC, we observed a clear excimer emission that allowed us to follow the concentration dependence of the excimer formation. Pyrene-labeled gangliosides are compared to pyrenyldecanoic acid and pyrene-labeled phosphatidylcholine (Figure 4A). In the fluid phase the curves obtained with pyrene-labeled gangliosides exhibit an upward deflection in the I_D/I_M vs. concentration curves, but only at high probe concentration. However, we do not believe that this is due to a phase separation within pyrene-labeled ganglioside containing DPPC vesicles. From the analytical studies we know that, up to 6 mol %, pelleted vesicles contain exactly the amount of labeled ganglioside that was added during the preparation. At higher concentrations we observed the segregation of small vesicles or mixed ganglioside–phospholipid micelles into the supernatant of the centrifuged probe. These structures exhibit increased ganglioside content and lead to higher average I_D/I_M values in the original vesicle preparation, which was used for the fluorescence measurement.

Low Ca^{2+} concentrations (<10 mM) do not show any observable effect. At 200 mM Ca^{2+} slightly upward bending curves were obtained for all ganglioside labels (Figure 4B). However, the efficiency of Ca^{2+} to segregate gangliosides in the fluid PC phase is extremely low and is, as will be discussed later, caused only by the Ca^{2+}-induced stabilization of the DPPC membrane.

From the experiments shown so far we can exclude an aggregation of gangliosides via Ca^{2+} bridges. We have clear evidence that gangliosides differ considerably from other negatively charged lipids. In mixed PC–phosphatidic acid membranes, for example (Galla & Sackmann, 1975), and also in PC–phosphatidylserine mixtures (Ito et al., 1975), Ca^{2+} ions induced a complete phase separation. By the use of the excimer technique, an almost 10-fold increase of the I_D/I_M ratio was observed in a phosphatidic acid membrane containing 10 mol % pyrene-labeled phosphatidylcholine, after the addition of Ca^{2+} equimolar to the charged lipid. In the fluid state of the membrane we are able to calculate the diffusion coefficient from the linear part of the I_D/I_M vs. concentration curves. As was reported earlier, the lateral diffusion coefficient of PyPC is lower than that of PyC_{10} due to the difference in the molecular weight (Galla et al., 1979). The ceramide part of the gangliosides, however, is not that different from the diacylglycerol part of a phosphatidylcholine molecule. Neglecting the oligosaccharide part that may protrude out into the water, we expect comparable diffusion coefficients. This is almost true for PyG_{M3} and PyG_{M1}, whereas PyG_{D1a} and PyG_{D1b} have a slightly lower diffusion coefficient.

This is interesting in the light of a paper published by Maggio et al. (1980), who derived a structural model of G_{D1a}–PC complexes where the oligosaccharide part carrying the sialic acid residue envelops the phosphatidylcholine head group. Such a structural arrangement might slow down the lateral diffusion of the ganglioside PyG_{D1a} or PyG_{D1b} in PC membranes. Goins et al. (1986) reported that ganglioside diffusion is reduced due to an additional hydrodynamic drag caused by the bulky head group. However, from photobleaching experiments (Kapitza & Rüppel, 1984) comparing glycoprotein and lipid diffusion, we know that the lateral diffusion of a solute in a bilayer membrane is mainly determined by the membrane-bound part. Diffusion coefficients of lipids and proteins are comparable in size, thus excluding a hydrodynamic drag from the water phase, at least in model membranes, because of the low viscosity of water compared to the viscosity in the hydrophobic membrane interior.

The difference between the diffusion coefficient determined in this paper, $D_{diff} = 1.6 \times 10^{-7}$ cm^2/s, and the one obtained by Goins et al. (1986) from photobleaching experiments using eosin-labeled gangliosides ($D_{diff} = 5 \times 10^{-9}$ cm^2/s) comes most likely from the different techniques. The latter value is in excellent agreement with other authors also using photobleaching to measure diffusion of fluorescein (Reidler et al., 1978) or rhodamine-labeled gangliosides (Spiegel et al., 1984). But finally it must be noted that diffusion coefficients determined by the excimer technique are always by a factor of 10 larger than those obtained by photobleaching recovery (Galla & Hartmann, 1980; Fahey & Webb, 1978). It seems that the comparison of absolute values obtained under different conditions and with different techniques is not justified. Despite this discrepancy we are able to exclude by our experiments both the formation of tight PC–ganglioside complexes and a hydrodynamic drag acting on the oligosaccharide head group.

The observed Ca^{2+} effect is in excellent agreement with results reported by Goins et al. (1986). We have clearly demonstrated that, even at high concentrations, Ca^{2+} ions do not significantly alter the lateral diffusion, therefore excluding a possible effect of cross-bridged ganglioside molecules, even in the presence of Ca^{2+} up to 200 mM.

From the thermotropic phase transition curves it is possible to gain information on the lateral distribution of the pyrene-labeled lipid components, especially in the phase-transition region where fluid and rigid lipid domains coexist. The lateral distribution of an excimer-forming probe is related to the local probe concentration that differs from the total probe concentration in a phase-separated system. The I_D/I_M value, on the other hand, depends on the local concentration of the pyrene probe. Very recently Hresko et al. (1986) analyzed phase-transition curves obtained by the excimer technique. A typical phase-transition curve, shown in Figure 5A, for DPPC membranes doped with PyPC is characterized by a maximum I_D/I_M value in the temperature range of the $P_{\beta'}$ phase and a distinct decrease of the excimer yield with increasing temperature at the host lipid phase transition. Curves like this have been reported ever since the application of the excimer technique to studying physical and structural properties of lipid bilayer membranes (Galla & Sackmann, 1974, 1975; Müller et al., 1986). Hresko et al. (1986) interpreted the I_D/I_M vs. temperature curves of PyPC in DPPC membranes by a random distribution of the probe molecules in pure gel and in pure fluid DPPC bilayers. In the phase-transition region, however, PyPC molecules preferentially distribute in the fluid phase, leading to the drop in I_D/I_M at the phase transition. From simulated I_D/I_M vs. temperature curves, the experimental curve was found to fit the shape of that for a system with complete miscibility but nonideal mixing between the pyrene probe and the host lipid.

A completely different shape of the phase-transition curve was obtained in DMPC membranes, again with PyPC as a probe molecule (Figure 5B). In complete agreement with Hresko et al. (1986), the phase-transition region is now determined only by a small plateau of the I_D/I_M ratio. This phase-transition curve resembles the theoretical curve for a system with nearly ideal mixing, which means that the probe distributes equally between the fluid and the gel domains of the bilayer membrane.

To recapitulate, the larger the height of the I_D/I_M peak just below the phase transition is, the larger the preference of the probe for the fluid state is. With regard to the effect of Ca^{2+}, in pure DPPC membranes a Ca^{2+} concentration of 200 mM induces an upward shift of the phase-transition temperature by about 2 °C and an increase in the peak height just below the phase transition. In terms of the perceding discussion this means that tightening the DPPC membrane increases the preference of the PyPC probe for the fluid bilayer or decreases its solubility in the gel membrane domains that are further rigidified by Ca^{2+} ions. In DMPC membranes Ca^{2+} ions do not induce such a drastic change (Figure 5B), clearly demonstrating the inability of Ca^{2+} to disturb almost ideally mixed membranes made of lipid components with low and equal affinity for Ca^{2+} ions (McDaniel & McLaughlin, 1985). We measured phase-transition curves of DPPC membranes using pyrene-labeled gangliosides PyG_{M3} (Figure 6), PyG_{M2}, PyG_{M1}, and PyG_{D1a} (Figure 8) as probe molecules. The effect of Ca^{2+} up to 200 mM is demonstrated (open symbols in Figures 6–8). Phase-transition curves taken at different pyrene-labeled ganglioside concentrations up to 5 mol % yield the same results. Therefore, we can exclude artifacts caused by the labeled molecules in the concentration range under investigation.

With PyG_{M3} as a probe molecule in a medium concentration range between 2 and 6 mol % and in the absence of Ca^{2+}, the I_D/I_M vs. temperature curves exhibit a plateau instead of a peak in the phase-transition region, which is similar to the shape of the DMPC phase-transition curve. The mixture is nonideal but not too far removed from ideal. Phase-transition curves obtained with PyG_{M2} (Figure 8) are somewhat nearer to ideality. The distribution behavior of PyG_{M1} follows this line, exhibiting an almost continuous increase in the I_D/I_M values. This system is therefore close to an ideal mixture. The phase-transition curve obtained with PyG_{D1a} exhibits a discontinuity with a steplike increase in the I_D/I_M ratio at the host lipid phase transition. This shape resembles the theoretical curve for an ideal mixture.

Ca^{2+} ions are able to recover the I_D/I_M peak in PyG_{M3}-doped membranes but less so for PyG_{M2} and hardly at all for PyG_{M1}. In PyG_{D1a}- or PyG_{D1b}-containing DPPC membranes a peak could not be recovered. The continuous growth of the I_D/I_M peak with Ca^{2+} concentration obtained with PyG_{M3} is shown in Figure 7.

We conclude that, in the absence of Ca^{2+}, gangliosides form almost ideal mixtures with phosphatidylcholines. This is most pronounced with disialogangliosides. Ca^{2+} is able to induce a ganglioside preference for the fluid phase. However, this should not be used as an argument for a ganglioside–Ca^{2+} interaction but rather for a solid phase immiscibility induced by the tightening of the PC membrane. A passive exclusion of the ganglioside from gel-phase domains is a consequence of the Ca^{2+}–DPPC interaction. If the system approaches ideality of mixing, Ca^{2+} is not able to induce such a preference for fluid domains. From our experiments we can rule out a significant interaction and especially a chelating effect of Ca^{2+} on gangliosides in DPPC membranes. This result supports the finding of McDaniel and McLaughlin (1985), who reported that Ca^{2+} binds to gangliosides as weakly as to phospholipids with an association constant of less than 100 M^{-1}. We also share their opinion that the idea of gangliosides serving as distinct Ca^{2+} receptors, or for storage of Ca^{2+} ions, is still open to question.

Registry No. DPPC, 63-89-8; DMPC, 18194-24-6; Ca, 7440-70-2; 12-(1-pyrenyl)dodecanoate *N*-succinimidyl ester, 99225-96-4; 12-(1-pyrenyl)dodecanoic acid, 69168-45-2; *N*-hydroxysuccinimide, 6066-82-6.

REFERENCES

Birks, J. B., Dyson, D. J., & Munro, I. H. (1963) *Proc. R. Soc. London, A 275*, 575–588.

Bremer, E. G., Hakomori, S., Bowen-Pope, D. F., Rainers, E., & Ross, R. (1984) *J. Biol. Chem. 259*, 6818–6825.

Chen, P. S., Toribara, T. Y., & Warner, H. (1956) *Anal. Chem. 28*, 1756–1758.

Conzelmann, E., & Sandhoff, K. (1978) *Proc. Natl. Acad. Sci. U.S.A. 75*, 3979–3983.

Corti, M., Degiorgio, V., Ghidoni, R., Sonnino, S., & Tettamanti, G. (1980) *Chem. Phys. Lipids 26*, 225–238.

Fahey, P. F., & Webb, W. W. (1978) *Biochemistry 17*, 3046–3053.

Folch, J., Lees, M. B., & Sloane Stanley, G. H. (1957) *J. Biol. Chem. 226*, 497–509.

Formisano, S., Johnson, M. L., Lee, G., Aloy, S. M., & Edelhoch, H. (1979) *Biochemistry 18*, 1119–1124.

Förster, T. (1969) *Angew. Chem. 81*, 364–374.

Galla, H.-J., & Sackmann, E. (1974) *Biochim. Biophys. Acta 339*, 103–115.

Galla, H.-J., & Sackmann, E. (1975) *J. Am. Chem. Soc. 97*, 4114–4120.

Galla, H.-J., & Hartmann, W. (1980) *Chem. Phys. Lipids 27*, 199–219.

Galla, H.-J., & Hartmann, W. (1981) *Methods Enzymol. 72*, 471–479.

Galla, H.-J., Hartmann, W., Theilen, U., & Sackmann, E. (1979) *J. Membr. Biol. 48*, 215–236.
Gammack, D. B. (1963) *Biochem. J. 88*, 373–383.
Goins, B., & Freire, E. (1985) *Biochemistry 24*, 1791–1797.
Goins, B., Masserini, M., Barisas, B. G., & Freire, E. (1986) *Biophys. J. 49*, 849–856.
Hakomori, S. (1981) *Annu. Rev. Biochem. 50*, 733–764.
Hayashi, K., Mühleisen, M., Probst, W., & Rahmann, H. (1984) *Chem. Phys. Lipids 34*, 317–322.
Hresko, R. C., Sugar, J. P., Barenholz, Y., & Thompson, T. E. (1986) *Biochemistry 25*, 3813–3828.
Ito, T., Ohnishi, S., Ishinaga, M., & Kito, M. (1975) *Biochemistry 14*, 3064–3069.
Kapitza, H. G., & Rüppel, D. A. (1984) *Biophys. J. 45*, 577–587.
Lapidot, Y., Rappaport, S., & Wolman, Y. (1967) *J. Lipid Res. 8*, 142–145.
Lazarovici, P., & Yavin, E. (1985) *Biochim. Biophys. Acta 812*, 523–531.
Ledeen, R. W., & Yu, R. K. (1982) *Methods Enzymol. 83*, 139–143.
Maggio, B., Cumar, F. A., & Caputto, R. (1980) *Biochem. J. 189*, 435–440.
Masserini, M., & Freire, E. (1986) *Biochemistry 25*, 1043–1049.
McDaniel, R., & McLaughlin, S. (1985) *Biochim. Biophys. Acta 819*, 153–160.
Momoi, T., Ando, S., & Nagai, Y. (1976) *Biochim. Biophys. Acta 441*, 488.
Mraz, W., Schwarzmann, G., Sattler, J., Momoi, T., Seemann, B., & Wiegandt, H. (1980) *Hoppe-Seyler's Z. Physiol. Chem. 361*, 177–185.
Müller, H.-J., Luxnat, M., & Galla, H.-J. (1986) *Biochim. Biophys. Acta 856*, 283–289.
Neuenhofer, S., Schwarzmann, G., Egge, H., & Sandhoff, K. (1985) *Biochemistry 24*, 525–532.
Peters, M. W., Mehlhorn, J. E., Barber, K. R., & Grant, C. W. M. (1984) *Biochim. Biophys. Acta 778*, 419–428.
Rahmann, H., & Hilbig, R. (1983) *J. Comp. Physiol. 151*, 215–224.
Reidler, J., Eldridge, C., Schlessinger, Y., Elson, E., & Wiegandt, H. (1978) *J. Supramol. Struct. Suppl. 2*, 306a.
Schwarzmann, G. (1978) *Biochim. Biophys. Acta 529*, 106–114.
Schwarzmann, G., & Sandhoff, K. (1987) *Methods Enzymol. 138*, 319–341.
Sela, B. A., & Bach, D. (1984) *Biochim. Biophys. Acta 771*, 177–182.
Shichijo, S., & Alving, C. R. (1986) *Biochim. Biophys. Acta 858*, 118–124.
Somerharju, P. J., Virtanen, J. A., Edlund, K. K., Vainio, P., & Kinnunen, P. K. J. (1985) *Biochemistry 24*, 2773–2781.
Spiegel, S. (1985) *Biochemistry 24*, 5947–5952.
Spiegel, S., Schlessinger, J., & Fishman, P. H. (1984) *J. Cell Biol. 99*, 699–704.
Stahl, E., & Kaltenbach, U. (1961) *J. Chromatogr. 5*, 351–356.
Svennerholm, L. (1957) *Biochim. Biophys. Acta 24*, 604–611.
Svennerholm, L. (1963) *J. Neurochem. 10*, 613–623.
Svennerholm, L. (1972) *Methods Carbohydr. Chem. 6*, 464.
Thompson, T. E., Allietta, M., Brown, R. E., Johnson, M. L., & Tillack, T. W. (1985) *Biochim. Biophys. Acta 817*, 229–237.
Trams, H. C., & Lauter, C. J. (1962) *Biochim. Biophys. Acta 60*, 350–358.
Wiener, J. R., Pal, R., Barenholz, Y., & Wagner, R. R. (1985) *Biochemistry 24*, 7651–7658.
Wong, M., Brown, R. E., Barenholz, Y., & Thompson, T. E. (1984) *Biochemistry 23*, 6498–6505.
Yohe, H. C., & Rosenberg, A. (1972) *Chem. Phys. Lipids 9*, 279–294.
Yohe, H. C., Roark, D. E., & Rosenberg, A. (1976) *J. Biol. Chem. 251*, 7085–7087.

CORRECTIONS

Biotin-Dependent Carboxylation Catalyzed by Transcarboxylase Is a Stepwise Process, by Stephen J. O'Keefe and Jeremy R. Knowles*, Volume 25, Number 20, October 7, 1986, pages 6077–6084.

Page 6080. In column 1, the last sentence should read as follows: F was determined for each time point as 2(dpm in malonyl-CoA)/(total dpm recovered), since the concentrations of the thioesters were equal. In column 2, under Velocity of the Thioester Exchange Reaction, the third sentence should read as follows: The average rate for the exchange reaction was 0.137 μmol mL^{-1} min^{-1}.

Inhibition of Protein Cross-Linking in Ca^{2+}-Enriched Human Erythrocytes and Activated Platelets, by L. Lorand,* N. Barnes, J. A. Bruner-Lorand, M. Hawkins, and M. Michalska, Volume 26, Number 1, January 13, 1987, pages 308–313.

Page 312. The mechanism of enzyme inactivation is likely to include also the elimination of the amine moiety of the inhibitor:

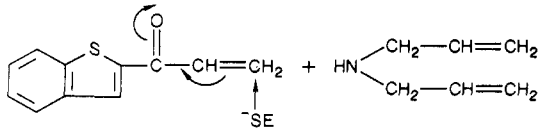

Influence of the Calcium-Induced Gel Phase on the Behavior of Small Molecules in Phosphatidylserine and Phosphatidylserine–Phosphatidylcholine Multilamellar Vesicles, by Kathryn I. Florine and Gerald W. Feigenson*, Volume 26, Number 6, March 24, 1987, pages 1757–1768.

Page 1764. Equation 7 should read

$$F = (F)_{LC} + \frac{[G]}{R_{LC/G}(1 - [G]) + [G]}[(F)_G - (F)_{LC}]$$

Protein Redistribution in Model Membranes: Clearing of M13 Coat Protein from Calcium-Induced Gel-Phase Regions in Phosphatidylserine/Phosphatidylcholine Multilamellar Vesicles, by Kathryn I. Florine and Gerald W. Feigenson*, Volume 26, Number 11, June 2, 1987, pages 2978–2983.

Page 2981. Equation 3 should read

$$F = F_{LC} + \frac{[G]}{R_{LC/G}(1 - [G]) + [G]}(F_G - F_{LC})$$